

QUANTUM CHEMICAL SIMULATION OF MoO₃ DISPERSION ON HYDROXYLATED SiO₂ SURFACE

Nasiedkin D.B., Nazarchuk M.O., Grebenyuk A.G., Sharanda L.F., Plyuto Yu.V.

*Chuiko Institute of Surface Chemistry, National Academy of Sciences of Ukraine,
General Naumov Str. 17, Kyiv 03164, Ukraine e-mail: nasiedkindm@gmail.com*

The aim of the present work is to evaluate the energetic favourability of the formation of different molybdate species ($\equiv\text{Si-O-})_2\text{Mo(=O)}_2$ and $\text{=Si(-O-)}_2\text{Mo(=O)}_2$ during the thermally induced MoO₃ dispersion on hydroxylated SiO₂ surface. In order to do this a quantum chemical modelling of the reaction $\text{O}_{12}\text{Si}_{10}(\text{OH})_{16} + \text{MoO}_3 = \text{O}_{12}\text{Si}_{10}(\text{OH})_{14}\text{O}_2\text{MoO}_2 + \text{H}_2\text{O}$ within the temperature interval of 300–1100 K was undertaken using the Restricted Hartree-Fock method (the LCAO approximation) with the SBKJC (Stevens-Basch-Krauss-Jasien-Cundari) valence basis set. The cluster $\text{O}_{12}\text{Si}_{10}(\text{OH})_{16}$ which represents a structural fragment of a β -cristobalite crystal was used in this work as a model of highly hydroxylated silica surface.

We considered two structures of molybdate ($\equiv\text{Si-O-})_2\text{Mo(=O)}_2$ species attached to $\text{O}_{12}\text{Si}_{10}(\text{OH})_{16}$ silica cluster via silanol groups. Molybdate species ($E_{\text{tot}} -584.60147$ Hartree) attached to silica cluster via distant silanols appeared more energetically favourable than molybdate species ($E_{\text{tot}} -584.56565$ Hartree) attached to silica cluster via nearby silanols. The energy of molybdate $\text{=Si(-O-)}_2\text{Mo(=O)}_2$ species ($E_{\text{tot}} -584.48399$ Hartree) attached to $\text{O}_{12}\text{Si}_{10}(\text{OH})_{16}$ silica cluster via silanediol group is less favourable energetically in comparison with those attached via silanol groups because of higher bond angle straining.

The reaction $\text{O}_{12}\text{Si}_{10}(\text{OH})_{16} + \text{MoO}_3 = \text{O}_{12}\text{Si}_{10}(\text{OH})_{14}\text{O}_2\text{MoO}_2 + \text{H}_2\text{O}$ in the temperature interval of 300–1100 K which simulates by quantum chemical calculations the dispersion of MoO₃ on hydroxylated SiO₂ surface was found to be energetically favourable. The experimentally optimised temperature of ca. 800 K required for dispersion of MoO₃ on hydroxylated SiO₂ surface is determined by MoO₃ evaporation and transportation via the gas phase.

Keywords: silica, molybdena, thermally induced dispersion, thermal spreading, supported heterogeneous catalysts, quantum chemical calculations.

Introduction

Nowadays, there is a standing interest in probing monomeric molybdate species on the surface of silica supports by experimental techniques [1–5] and theoretical methods [6, 7]. The distribution of MoO₃ on the surface of dispersed supports is important from fundamental and applied points of view as it plays a crucial role in the development of scientific basis of the rational design of supported heterogeneous catalysts in chemical and petrochemical industry and in environmental control. The process of catalytic metathesis of olefins is an example of the industrially important reaction where molybdate species in atomically precise form play a central role [8–10].

Numerous experimental studies of MoO₃ thermally induced dispersion over supports surface were undertaken [11]. They were focused on individual well defined SiO₂ [12, 13], Al₂O₃ [13–16] or mixed SiO₂–Al₂O₃ [17, 18] supports, siliceous [19–21] and aluminosilicate [15, 16, 22] molecular sieves. It was experimentally determined that the temperature of ca. 800 K is required for dispersion of MoO₃ over supports surface. Special attention was given to molybdate species resulted from MoO₃ loading on aluminosilicate molecular sieves MCM-22, MCM-56 and

2D-MFI [23] and on siliceous molecular sieves MCM-41, MCM-48 and SBA-15 [24, 25] which are active in olefins metathesis.

The driving force for the bulk MoO₃ spreading is the surface free energy which is lower for surface-dispersed species. Stabilisation of molybdena surface species occurs due to interaction with surface hydroxyl groups [11]. In the case of dispersed supports like Al₂O₃, SiO₂ or TiO₂ the gas phase diffusion mechanism where Mo oxide clusters are evaporated from MoO₃ crystallites with subsequent dispergation in monomeric state on the support surface was proposed [26, 27]. The diffusion process of MoO₃ on oxide thin films (Al₂O₃, SiO₂, TiO₂) was also investigated. During thermal treatment, MoO₃ diffused onto the surface of those films and formed a monolayer or a submonolayer. A possible explanation for all the phenomena is the combination of surface diffusion onto the surface of the support and transportation via the gas phase [28, 29].

The aim of the present work is to evaluate the energetic favourability of the formation of different molybdate species ($\equiv\text{Si-O-})_2\text{Mo(=O)}_2$ and $=\text{Si(-O-)}_2\text{Mo(=O)}_2$ during the thermally induced MoO₃ dispergation on hydroxylated SiO₂ surface. In order to do this a quantum chemical modelling of the reaction $\text{O}_{12}\text{Si}_{10}(\text{OH})_{16} + \text{MoO}_3 = \text{O}_{12}\text{Si}_{10}(\text{OH})_{14}\text{O}_2\text{MoO}_2 + \text{H}_2\text{O}$ within the temperature interval of 300–1100 K was undertaken.

Research methods

The process of interaction between MoO₃ and silica surface was simulated using the Restricted Hartree-Fock method (the LCAO approximation) with the Firefly QC package [30] which is partially based on the GAMESS (US) [31] source code. In order to shorten the computing time, the SBKJC (Stevens-Basch-Krauss-Jasien-Cundari) valence basis set was used which required application of respective effective core potential. The values of the Gibbs energy (ΔG) for the considered species were calculated within 300–1100 K temperature interval using the ideal gas, rigid rotor, harmonic normal mode approximations and the pressure $P = 101.325$ kPa as the sum of electronic energy, zero point energy, and the energy contributions of vibrational, rotational, and translational movements.

Results and discussion

The cluster $\text{O}_{12}\text{Si}_{10}(\text{OH})_{16}$ (Fig. 1) was used in this work as a model of highly hydroxylated silica surface. The cluster starting geometry proposed in [32, 33] represents a structural fragment of a β -cristobalite crystal. Silicon atom in the core siloxane chains are saturated by four silanol and six silanediol groups.

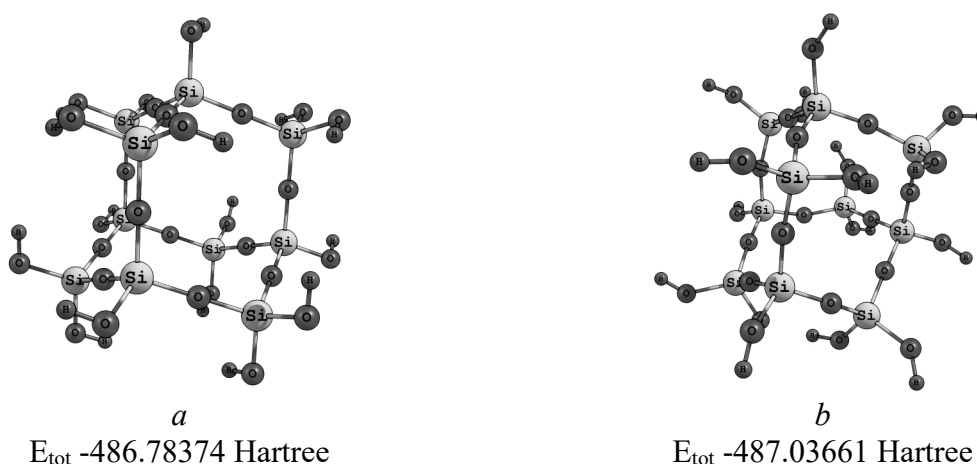


Fig. 1. The structure and energy of $\text{O}_{12}\text{Si}_{10}(\text{OH})_{16}$ cluster with starting (*a*) and optimised (*a*) geometry

Such $\text{O}_{12}\text{Si}_{10}(\text{OH})_{16}$ cluster was considered as providing a realistic structure for the SiO_2 surface and exhibiting high stability due to its large size [34]. It presents on its surface different types of hydroxyl groups that can act as adsorption and reactions sites and is also useful to model silica gel surface [35].

In the initial $\text{O}_{12}\text{Si}_{10}(\text{OH})_{16}$ model composed of regular SiO_4 tetrahedra (Fig. 1, *a*), all Si-O bonds had the lengths of 1.700 Å and O-Si-O angles of 109.5° [36, 37]. After the geometry optimisation (Fig. 1, *b*), they have slightly changed to 1.631–1.651 Å and 104.5–108.2°, respectively. The total energy of the cluster with optimised structure (Fig. 1, *b*) of -0.25286 Hartree was less than the starting model (Fig. 1, *a*) confirming its adequate selection.

The optimised geometry of MoO_3 molecule ($E_{\text{total}} = -114.23859$ Hartree) of C_{3v} symmetry has the Mo=O bond length of 1.708 Å and the bond angle O=Mo=O of 114.9°. It appears to be close to experimental values of MoO_3 molecule of C_{3v} symmetry with the bond length of 1.711±0.008 Å and the bond angle O=Mo=O of 112±8° obtained from the electron diffraction investigation in the vapour phase [38]. A pyramidal C_{3v} structure for gaseous MoO_3 was also suggested from the infrared spectrum [39] with a Mo=O bond length of 1.73 Å.

The calculated values of geometric parameters of MoO_3 model are close to the analogous values obtained earlier. HF SCF calculations [40] yielded a Mo=O bond length of 1.682 Å and showed that the molecule is nonplanar with Mo=O bonds forming an angle of 105° with the C_3 axis. After correlation corrections, the values 1.766 Å and 112°, respectively, were obtained for these parameters. By DFT calculations, a Mo=O bond length was found to be of 1.734 Å and the bond angle O=Mo=O of 108.0° [41].

We considered two structures of molybdate ($\equiv\text{Si-O-})_2\text{Mo(=O)}_2$ species attached to $\text{O}_{12}\text{Si}_{10}(\text{OH})_{16}$ silica cluster via silanol groups (Fig. 2). The structure **a** corresponds to the molybdate species attached to silica cluster via nearby silanols while structure **b** corresponds to the molybdate species attached to silica cluster via distant silanols. The structure **b** appeared to be more energetically favourable ($E_{\text{tot}} -584.56565$ Hartree) in contrast to structure **a** ($E_{\text{tot}} -584.60147$ Hartree).

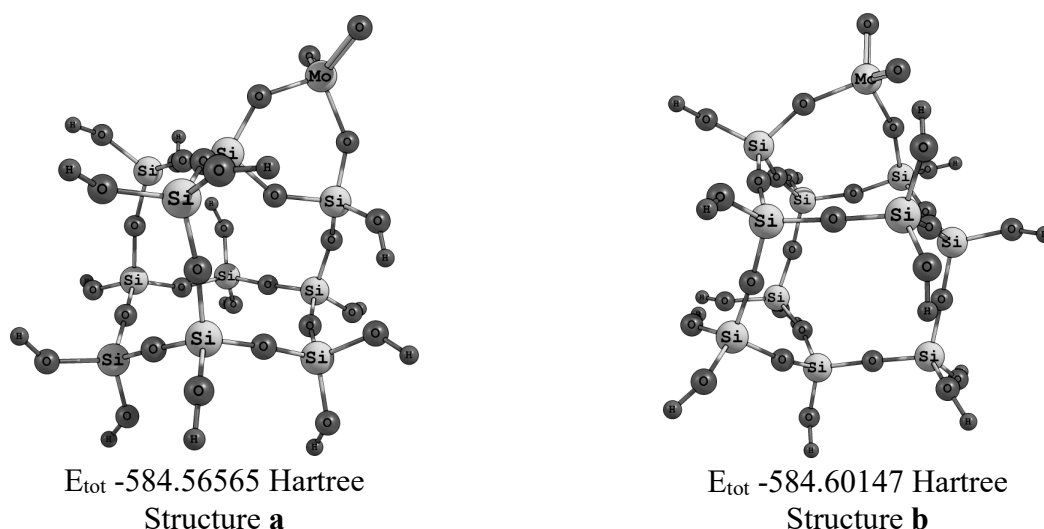
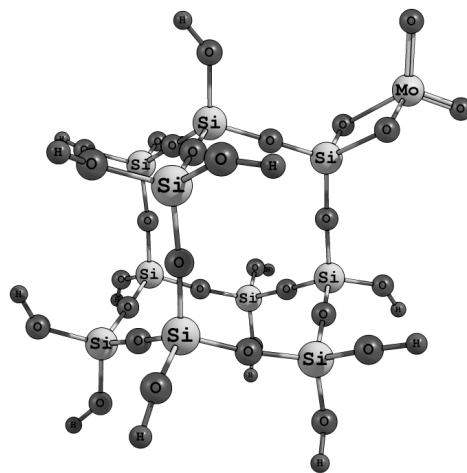


Fig. 2. Geometry-optimised structures of molybdate ($\equiv\text{Si-O-})_2\text{Mo(=O)}_2$ species attached to $\text{O}_{12}\text{Si}_{10}(\text{OH})_{16}$ silica cluster via silanol groups

The Mo=O bond length in molybdate ($\equiv\text{Si-O-})_2\text{Mo(=O)}_2$ species **a** and **b** is almost the same and varies in the range of 1.683–1.685 Å. This also concerns the O=Mo=O angle which is in the range of 108.8–109.0° and is very close to theoretical value of 109.5° in tetrahedral coordination. The main difference is observed for O-Mo-O angle in molybdate ($\equiv\text{Si-O-})_2\text{Mo(=O)}_2$ species which for the structures **a** and **b** was found to be of 94.8° and 102.0°,

correspondingly. The observed O-Mo-O angle in the structures **a** appeared to be more distorted in comparison with that in the structures **b**. This correlates with higher energetic favourability of the structure **b** in comparison with the structure **a** due to a less bond angle straining.

The optimised structure of molybdate $=\text{Si}(-\text{O}-)_2\text{Mo}(=\text{O})_2$ species (structure **c**) attached to $\text{O}_{12}\text{Si}_{10}(\text{OH})_{16}$ silica cluster via silanediol group is shown in Fig. 3.



E_{tot} -584.48399 Hartree

Structure **c**

Fig. 3. Geometry-optimised structure of molybdate $=\text{Si}(-\text{O}-)_2\text{Mo}(=\text{O})_2$ species attached to $\text{O}_{12}\text{Si}_{10}(\text{OH})_{16}$ silica cluster via silanediol group

The energy of molybdate $=\text{Si}(-\text{O}-)_2\text{Mo}(=\text{O})_2$ species (structure **c**) attached to $\text{O}_{12}\text{Si}_{10}(\text{OH})_{16}$ silica cluster via silanediol group is of -584.48399 Hartree. It is higher than those of -584.56565 and -584.60147 Hartree of molybdate $(=\text{Si}-\text{O}-)_2\text{Mo}(=\text{O})_2$ species attached to silica cluster via silanol groups in the structures **a** and **b**. This means that molybdate $=\text{Si}(-\text{O}-)_2\text{Mo}(=\text{O})_2$ species (structure **c**) attached to $\text{O}_{12}\text{Si}_{10}(\text{OH})_{16}$ silica cluster via silanediol group is less favourable energetically in comparison with those attached via silanol groups.

The Mo=O bond length in molybdate $=\text{Si}(-\text{O}-)_2\text{Mo}(=\text{O})_2$ species (structure **c**) is 1.681 Å and almost coincides with those in the structures **a** and **b** which are in the range of 1.683–1.685 Å. This also concerns the O=Mo=O angle of 109.2° which is close to that of 108.8–109.0° of the structure **a** and **b** and correspond to theoretical value of 109.5° in tetrahedral coordination.

In contrast, O-Mo-O angle in molybdate $=\text{Si}(-\text{O}-)_2\text{Mo}(=\text{O})_2$ species of the structure **c** was found to be close to 77.0°. It appears even more distorted in comparison with that in the structures **a**. This correlates with lower energetic favourability of the structure **c** (E_{tot} -584.48399 Hartree) in comparison with the structure **a** (E_{tot} -584.56565 Hartree) due to higher bond angle straining.

The temperature dependences of the Gibbs energy of the reaction $\text{O}_{12}\text{Si}_{10}(\text{OH})_{16} + \text{MoO}_3 = \text{O}_{12}\text{Si}_{10}(\text{OH})_{14}\text{O}_2\text{MoO}_2 + \text{H}_2\text{O}$ which can result in the formation of different surface molybdate species $(=\text{Si}-\text{O}-)_2\text{Mo}(=\text{O})_2$ and $=\text{Si}(-\text{O}-)_2\text{Mo}(=\text{O})_2$ was calculated and presented in Fig. 4.

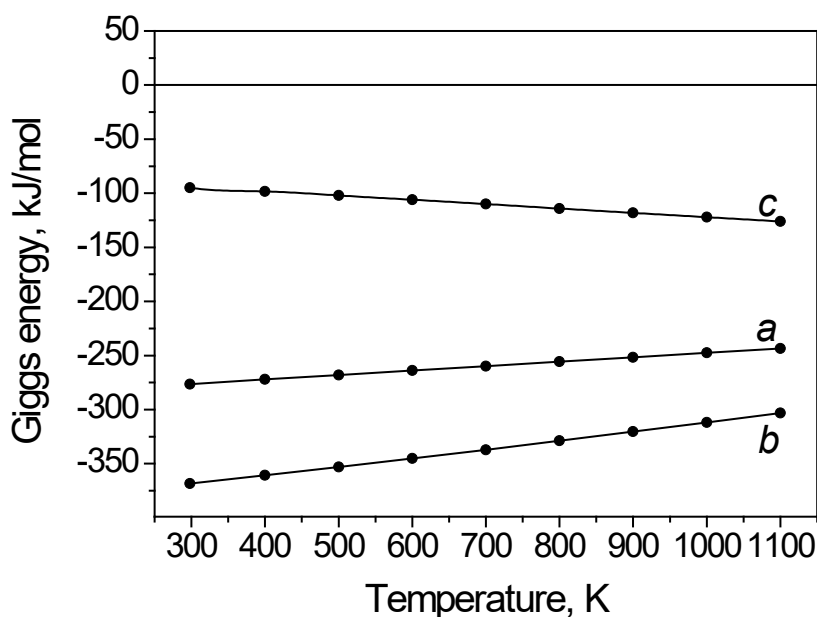


Fig. 4. The temperature dependence of the Gibbs energy for the reaction of MoO₃ molecule with O₁₂Si₁₀(OH)₁₆ cluster resulting in the formation of surface molybdate species (≡Si-O-)₂Mo(=O)₂ (*a* and *b*) and =Si(-O-)₂Mo(=O)₂ (*c*)

All considered processes were found to be energetically favourable in the temperature interval of 300–1100 K. The value of the Gibbs energy of MoO₃ reaction with silanol groups resulted in the structure **a** formation varies from -276 to -243 kJ/mol. The formation of the structure **b** also resulted from MoO₃ reaction with silanol groups was found even more preferable and varies in the range from -368 to -303 kJ/mol. In contrast, the formation of the structure **c** resulted from MoO₃ reaction with silanediol groups is less preferable and varies from -95 to -126 kJ/mol. The observed behaviour of silanol and silanediol groups in the reaction with MoO₃ in the temperature interval of 300–1100 K agrees with the calculated values of the E_{tot} -584.56565, -584.60147 and -584.48399 Hartree for the structures **a**, **b** and **c**, correspondingly, and the high bond angle straining in the structure **c**. The considered processes were found to be energetically favourable in the temperature interval of 300–1100 K. Therefore, it is reasonable to assume that the experimentally optimised temperature of ca. 800 K required for dispergation of MoO₃ is determined by its evaporation and transportation via the gas phase over SiO₂ surface to reach the silanol and silanediol groups. This agrees with experimental observations of evaporation of molybdenum oxide clusters from MoO₃ crystallites with subsequent dispergation in monolayer or a submonolayer state on the surface of Al₂O₃, SiO₂ or TiO₂ in the bulk [26, 27] or thin film [28, 29] form.

Conclusions

The reaction O₁₂Si₁₀(OH)₁₆ + MoO₃ = O₁₂Si₁₀(OH)₁₄O₂MoO₂ + H₂O in the temperature interval of 300–1100 K which simulates by quantum chemical calculations the dispergation of MoO₃ on hydroxylated SiO₂ surface was found to be energetically favourable.

The formation molybdate =Si(-O-)₂Mo(=O)₂ species attached to O₁₂Si₁₀(OH)₁₆ silica cluster via silanediol group is less favourable with respect to molybdate (≡Si-O-)₂Mo(=O)₂ species attached to O₁₂Si₁₀(OH)₁₆ silica cluster via silanol groups because of higher bond angle straining.

The experimentally optimised temperature of ca. 800 K required for dispersion of MoO₃ on hydroxylated SiO₂ surface is determined by MoO₃ evaporation and transportation via the gas phase.

Acknowledgement

The research was partially supported by the Integrated Targeted Research Programme “Fundamental Problems of Developing Novel Substances and Materials of Chemical Production” of the National Academy of Sciences of Ukraine.

References

1. Pampararo G., Garbarino G., Ardoino N., Riani P., Busca G. A study of molybdena catalysts in ethanol oxidation. Part 1. Unsupported and silica-supported MoO₃. *Chemical Technology and Biotechnology*. 2021. **96**(12): 3293. <https://doi.org/10.1002/jctb.6877>
2. Li L., Scott S.L. X-ray Absorption Spectroscopy Investigation into the Origins of Heterogeneity in Silica-Supported Dioxomolybdates. *J. Phys. Chem. C*. 2021. **125**(42): 23115. <https://doi.org/10.1021/acs.jpcc.1c05559>
3. Amakawa K., Wang Y., Kröhnert J., Schlögl R., Trunschke A. Acid sites on silica-supported molybdenum oxides probed by ammonia adsorption: Experiment and theory. *Molecular Catalysis*. 2019. 478: 110580. <https://doi.org/j.mcat.2019.110580>
4. Wang Zh.-M., Liu L.-J., Xiang B., Wang Y., Lyu Y.-J., Qi T., Si Zh.-B., Yang H.-Q. Hu Ch.-W. The design and catalytic performance of molybdenum active sites on an MCM-41 framework for the aerobic oxidation of 5-hydroxymethylfurfural to 2,5-diformylfuran. *Catal. Sci. Technol.* 2019. **9**(3): 811. <https://doi.org/10.1039/C8CY02291G>
5. Guo C.S., Hermann K., Hävecker M., Thielemann J.P., Kube P., Gregoriades L.J., Trunschke A., Sauer J., Schlögl R. Structural Analysis of Silica-Supported Molybdena Based on X-ray Spectroscopy: Quantum Theory and Experiment. *J. Phys. Chem. C*. 2011. **115**(31): 15449. <https://doi.org/10.1021/jp2034642>
6. Handzlik J., Kurlito K., Gierada M. Computational Insights into Active Site Formation during Alkene Metathesis over a MoO_x/SiO₂ Catalyst: The Role of Surface Silanols. *ACS Catal.* 2021. **11**: 13575. <https://doi.org/10.1021/acscatal.1c03912>
7. Kurlito K., Tielens F., Handzlik J. Isolated Molybdenum(VI) and Tungsten(VI) Oxide Species on Partly Dehydroxylated Silica: A Computational Perspective. *J. Phys. Chem. C*. 2020. **124**(5), 3002. <https://doi.org/10.1021/acs.jpcc.9b09586>
8. Fierro J.L.G., Mol J.C. Metathesis of Olefins on Metal Oxides. In: *Metal Oxides: Chemistry and Applications* (Boca Raton: CRC Press, 2006), pp 517–541. <https://doi.org/10.1201/9781420>
9. Bañares M.A., Mestl G. Chapter 2 Structural Characterization of Operating Catalysts by Raman Spectroscopy. *Advances in Catalysis*. 2009. **52**: 43. [https://doi.org/10.1016/S0360-0564\(08\)00002-3](https://doi.org/10.1016/S0360-0564(08)00002-3)
10. Lwin S., Wachs I.E. Olefin Metathesis by Supported Metal Oxide Catalysts. *ACS Catal.* 2014. **4**(8): 2505. <https://doi.org/10.1021/cs500528h>
11. Knözinger H., Taglauer E. 2.4.7 Spreading and Wetting. In: *Handbook of Heterogeneous Catalysis* (Weinheim: Wiley-VCH Verlag GmbH & Co. KgaA, 2008), pp 555–571. <https://doi.org/10.1002/9783527610044.hetcat0027>
12. Braun S., Appel L.G., Camorim V.L., Schmal M. Thermal Spreading of MoO₃ onto Silica Supports. *J. Phys. Chem. B*. 2000. **104**(28): 6584. <https://doi.org/10.1021/jp000287m>
13. Braun S., Appel L.G., Schmal M. Molybdenum species on alumina and silica supports for soot combustion. *Catalysis Communications*. 2005. **6**(1): 7. <https://doi.org/10.1016/j.catcom.2004.10.002>
14. Shi W., Cai X., Wei J., Ma J., Hu T., Wu N., Xie Y. EXAFS study of molybdenum oxide on the structure Al₂O₃. *Surf. Interface Anal.* 2001. **32**(1): 202. <https://doi.org/10.1002/sia.1037>
15. Mosqueira L., Fuentes G.A. Molecular selection of MoO_x species during migration on Al₂O₃ and zeolites Y and ZSM-5. *Molecular Physics*. 2002. **100**(19): 3055. <https://doi.org/10.1080/00268970210130173>

16. Mosqueira L., Gomez S.A., Fuentes G.A. Characterization of MoOx species on γ -Al₂O₃, Y and ZSM-5 zeolites during thermally activated solid–solid synthesis. *J. Phys.: Condens. Matter*. 2004. **16**(2): S2319. <https://doi.org/10.1088/0953-8984/16/22/034>
17. Debecker D.P., Stoyanova M., Rodemerck U., Eloy P., Léonard A., Su B.-L., Gaigneaux E.M. Thermal Spreading as an Alternative for the Wet Impregnation Method: Advantages and Downsides in the Preparation of MoO₃/SiO₂-Al₂O₃ Metathesis Catalysts. *J. Phys. Chem. C*. 2010. **114**(43): 18664. <https://doi.org/10.1021/jp1074994>
18. Debecker D.P., Stoyanova M., Rodemerck U., Gaigneaux E.M. Facile preparation of MoO₃/SiO₂-Al₂O₃ olefin metathesis catalysts by thermal spreading. In: *Studies in Surface Science and Catalysis*. **175**. Proc. 10th Int. Symp. (July 11–15, 2010, Louvain-la-Neuve, Belgium), pp 581–585. [https://doi.org/10.1016/S0167-2991\(10\)75113-2](https://doi.org/10.1016/S0167-2991(10)75113-2)
19. Li Zh., Gao L., Zheng Sh. Investigation of the dispersion of MoO₃ onto the support of mesoporous silica MCM-41. *Applied Catalysis A: General*. 2002. **236**(1–2): 163. [https://doi.org/10.1016/S0926-860X\(02\)00302-2](https://doi.org/10.1016/S0926-860X(02)00302-2)
20. Li Zh., Gao L., Zheng Sh. SEM, XPS, and FTIR studies of MoO₃ dispersion on mesoporous silicate MCM-41 by calcination. *Materials Letters*. 2003. **57**(29): 4605. [https://doi.org/10.1016/S0167-577X\(03\)00369-0](https://doi.org/10.1016/S0167-577X(03)00369-0)
21. Sampieri A., Pronier S., Blanchard J., Breysse M., Brunet S., Fajerweg K., Louis C., Pérot G. Hydrodesulfurization of dibenzothiophene on MoS₂/MCM-41 and MoS₂/SBA-15 catalysts prepared by thermal spreading of MoO₃. *Catalysis Today*. 2005. **107–108**: 537. <https://doi.org/10.1016/j.cattod.2005.07.069>
22. Mosqueira L., Angeles-Chavez C., Torres-García E. Thermal spreading of MoO₃ in H-ZY. *Materials Chemistry and Physics*. 2011. **126**(3): 930. <https://doi.org/10.1016/j.matchemphys.2010.12.006>
23. Balcar H., Kubů M., Žilková N., Shamzhy M. MoO₃ on zeolites MCM-22, MCM-56 and 2D-MFI as catalysts for 1-octene metathesis. *Beilstein J. Org. Chem*. 2018. **14**: 2931. doi:10.3762/bjoc.14.272
24. Balcar H., Topka P., Žilková N., Pérez-Pariente J., Čejka J. Metathesis of linear α -olefins with MoO₃ supported on MCM-41 catalyst. *Studies in Surface Science and Catalysis*. 2005. **156**: 795. [https://doi.org/10.1016/S0167-2991\(05\)80288-5](https://doi.org/10.1016/S0167-2991(05)80288-5)
25. Balcar H., Čejka J. Mesoporous Molecular Sieves as Supports for Metathesis Catalysts. In: Imamoglu Y., Dragutan V., Karabulut S. (eds) *Metathesis Chemistry*. NATO Science Series. **243**. Dordrecht: Springer, 2007), pp 151–166. https://doi.org/10.1007/978-1-4020-6091-5_9
26. Günther S., Gregoratti L., Kiskinova M., Taglauer E., Grotz P., Schubert U.A. Knözinger H. Transport mechanisms during spreading of MoO₃ on Al₂O₃ supports investigated by photoelectron spectromicroscopy. *The Journal of Chemical Physics*. 2000. **112**(12): 5440. <https://doi.org/10.1063/1.481111>
27. Günther S., Esch F., Gregoratti L., Barinov A., Kiskinova M., Taglauer E., Knözinger H. Gas-Phase Transport during the Spreading of MoO₃ on Al₂O₃ Support Surfaces: Photoelectron Spectromicroscopic Study. *J. Phys. Chem. B*. 2004. **108**(38): 14223. <https://doi.org/10.1021/jp031333w>
28. Xu W., Yan J., Wu N., Zhang H., Xie Y., Tang Y., Zhu Y., Yao W. Diffusing behavior of MoO₃ on Al₂O₃ and SiO₂ thin films. *Surface Science*. 2000. **470**(1–2): 121. [https://doi.org/10.1016/S0039-6028\(00\)00847-5](https://doi.org/10.1016/S0039-6028(00)00847-5)
29. Xu W., Xu J., Wu N., Yan J., Zhu Y., Huang Y., He W., Xie Y. Study of the diffusion behaviour of MoO₃ and ZnO on oxide thin films by SR-TXRF. *Surf. Interface Anal.* 2001. **32**(1): 301. <https://doi.org/10.1002/sia.1060>
30. Alex A. Granovsky, Firefly version 8. <http://classic.chem.msu.su/gran/firefly/index.html>.
31. Schmidt M.W., Baldrige K.K., Boatz J.A., Elbert S.T., Gordon M.S., Jensen J.H., Koseki S., Matsunaga N., Nguyen K.A., Su S., Windus T.L., Dupuis M., Montgomery J.A. General atomic and molecular electronic structure system. *J. Comput. Chem*. 1993. **14**(11): 1347. <https://doi.org/10.1002/jcc.540141112>

32. Khavryutchenko V., Sheka E. Computer modeling of amorphous silica structures. *React. Kinet. Catal. Lett.* 1993. **50**(1–2): 389. <https://doi.org/10.1007/BF02062241>
33. Khavryuchenko, V.D., Sheka, E.F. Computational modeling of amorphous silica. 2. Modeling the initial structures. *Aerosil. Journal of Structural Chemistry.* 1994. **35**(3): 291. <https://doi.org/10.1007/BF02578279>
34. Bounechada D., Darmastuti Zh., Andersson M., Ojamäe L., Spetz A.L., Skoglundh M., Carlsson P.-A. Vibrational Study of SO_x Adsorption on Pt/SiO₂. *J. Phys. Chem. C.* 2014. **118**(51): 29713. <https://doi.org/10.1021/jp506644w>
35. Qu R., Li C., Liu J., Xiao R., Pan X., Zeng X., Wang Z., Wu J. Hydroxyl Radical Based Photocatalytic Degradation of Halogenated Organic Contaminants and Paraffin on Silica Gel. *Environ. Sci. Technol.* 2018. **52**(13): 7220. <https://doi.org/10.1021/acs.est.8b00499>
36. Peacor, D. B. High-temperature single-crystal study of the cristobalite inversion. *Zeitschrift für Kristallographie – Crystalline Materials.* 1973. **138**(1–6): 274. <https://doi.org/10.1524/zkri.1973.138.jg.274>
37. Wright A.F., Leadbetter A.J. The structures of the β-cristobalite phases of SiO₂ and AlPO₄, *The Philosophical Magazine. A Journal of Theoretical Experimental and Applied Physics.* 1975. **31**(6):1391. <https://doi.org/10.1080/00318087508228690>
38. Spiridonov V.P., Zazorin E.Z. Modern High-Temperature Electron Diffraction. In *Characterization of High Temperature Vapors and Gases.* Proc. 10th Materials Research Symposium at the National Bureau of Standards, (September 18–22, 1978, Gaithersburg, Maryland). NBS Special Publication 561, Vol 1. U.S. Dep. of Commerce, Nat. Bureau of Standards, 1979, pp 711–755. <https://books.google.com.ua/books?id=OzpQ5yVtrxUC>
39. J. Phys. Chem. Ref. Data, Monograph 9. NIST-JANAF Thermochemical Tables. Part I and Part II. Fourth Edition (Chase M. W., Jr., Ed). National Institute of Standards and Technology, Gaithersburg, USA, 1998, p. 1593. <https://srdata.nist.gov/JPCRD/jpcrdM9.pdf>
40. Papakondylis A., Sautet Ph. Ab Initio Study of the Structure of the α-MoO₃ Solid and Study of the Adsorption of H₂O and CO Molecules on its (100). *Surface. J. Phys. Chem.* 1996. **100**(25): 10681. <https://doi.org/10.1021/jp953727w>
41. Zhou M., Andrews L. Infrared spectra and density functional calculations of the CrO₂⁻, MoO₂⁻, and WO₂⁻ molecular anions in solid neon. *The Journal of Chemical Physics.* 1999. **111**: 4230002E <https://doi.org/10.1063/1.479721>

КВАНТОВОХІМІЧНЕ МОДЕЛЮВАННЯ ПРОЦЕСУ ДИСПЕРГУВАННЯ MoO_3 НА ГІДРОКСИЛЬОВАНІЙ ПОВЕРХНІ SiO_2

Наседкін Д.Б., Назарчук М.О., Гребенюк А.Г., Шаранда Л.Ф., Плюто Ю.В.

*Інститут хімії поверхні ім. О.О. Чуйка Національної академії наук України,
вул. Генерала Наумова 17, Київ 03164, Україна, e-mail: nasiedkindm@gmail.com*

Метою даної роботи є оцінка енергетичної сприятливості утворення різних молібдатних груп ($\equiv\text{Si-O-}$) $_2\text{Mo(=O)}_2$ та $=\text{Si(-O-)}_2\text{Mo(=O)}_2$ під час термічно ініційованого диспергування MoO_3 на гідроксильованій поверхні SiO_2 . Для цього було здійснено квантовохімічне моделювання реакції $\text{O}_{12}\text{Si}_{10}(\text{OH})_{16} + \text{MoO}_3 = \text{O}_{12}\text{Si}_{10}(\text{OH})_{14}\text{O}_2\text{MoO}_2 + \text{H}_2\text{O}$ в температурному інтервалі 300–1100 К із використанням обмеженого методу Хартрі-Фока (наближення ЛКАО) з валентним базисом SBKJС (Stevens-Basch-Krauss-Jasien-Sundari). Кластер $\text{O}_{12}\text{Si}_{10}(\text{OH})_{16}$, який являє собою структурний фрагмент кристала β -кристобаліту, був використаний як модель високогідроксильованої поверхні кремнезему.

Ми розглянули дві структури молібдатних груп ($\equiv\text{Si-O-}$) $_2\text{Mo(=O)}_2$, прикріплених до кремнеземного кластера $\text{O}_{12}\text{Si}_{10}(\text{OH})_{16}$ через силанольні групи. Молібдатні групи ($E_{\text{tot}} - 584.60147$ Hartree), прикріплені до кремнеземного кластера через віддалені силанольні групи, виявляються більш енергетично вигідними, ніж молібдатні групи ($E_{\text{tot}} - 584.56565$ Hartree), прикріплені до кремнеземного кластера через сусідні силанольні групи. Енергія молібдатних груп $=\text{Si(-O-)}_2\text{Mo(=O)}_2$ ($E_{\text{tot}} - 584.48399$ Hartree), прикріплених до кремнеземного кластера $\text{O}_{12}\text{Si}_{10}(\text{OH})_{16}$ через силандіольні групи, менш енергетично вигідні в порівнянні з подібними групами, прикріпленими через силанольні групи, через більше напруження кута між зв'язками.

Знайдено, що реакція $\text{O}_{12}\text{Si}_{10}(\text{OH})_{16} + \text{MoO}_3 = \text{O}_{12}\text{Si}_{10}(\text{OH})_{14}\text{O}_2\text{MoO}_2 + \text{H}_2\text{O}$ в температурному інтервалі 300–1100 К, змодельована шляхом квантовохімічних розрахунків, свідчить, що процес диспергування MoO_3 на гідроксильованій поверхні SiO_2 є енергетично вигідним. Експериментальна оптимальна температура (близько 800 К), потрібна для диспергування MoO_3 на гідроксильованій поверхні SiO_2 , визначається випаровуванням та перенесенням MoO_3 в газовій фазі.

Keywords: *кремнезем, триоксид молібдену, термічно ініційоване диспергування, термічне розповсюдження, нанесені гетерогенні каталізатори, квантовохімічні розрахунки*